

Converting Chemically Functionalized Few-Layer Graphene to Diamond Films: A Computational Study

Liubov Yu. Antipina^{†,‡} and Pavel B. Sorokin^{*,†,§}

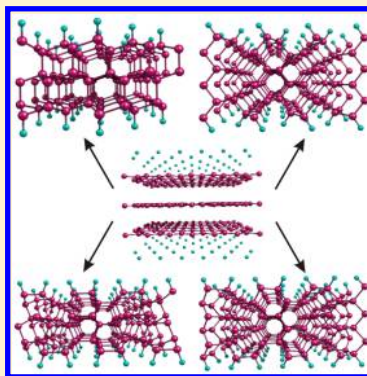
[†]Technological Institute for Superhard and Novel Carbon Materials, 7a Centralnaya Street, Troitsk, Moscow, 142190, Russian Federation

[‡]Moscow Institute of Physics and Technology, 9 Institutsky Lane, Dolgoprudny, 141700, Russian Federation

[§]National University of Science and Technology MISiS, 4 Leninskiy Prospekt, Moscow, 119049, Russian Federation

Supporting Information

ABSTRACT: We propose a new way to produce high-quality films of diamond from chemically functionalized few-layer graphene. Our ab initio calculations show that depending on functionalization few-layer graphene may convert spontaneously in a well-defined way to either cubic or hexagonal diamond films with a specific surface and well-defined properties. We provide specific results for the converting process using H, H₂, F, F₂, H₂O, and NH₃ as adsorbates at different temperatures and pressures.



INTRODUCTION

The isolation of graphene¹ opened a new field of two-dimensional materials in modern science. Pseudochiral Dirac's nature of the carriers, ballistic conductivity, and anomalous Hall effect² make graphene one of the most promising materials for science and advanced technology. The potential application of graphene in nanoelectronics can be enlarged by the functionalization, which leads to a significant change of the electronic, mechanical, and optical properties of this material. Graphene can be functionalized by various adatoms and molecular groups, for example, by hydrogen,^{3–9} fluorine,^{10–17} nitrogen,^{18,19} oxygen,^{20–23} etc.

Totally functionalized graphene can be considered as the first member in a series of sp³-bonded carbon films, whose conformers belong to the family of films with different surfaces. There are a number of reports^{24–26} on the possible existence of diamond films of nanometer thickness, the structure of which can be considered as chemically bonded neighboring graphene sheets. It was found^{7,26–29} that the multilayered graphene with adsorbed adatoms on the outer surfaces forms the diamond film without any activation barrier (at least for the films containing 2–6 layers), which was confirmed by a number of experimental data.^{8,10,20} In the ref 28, this effect was entitled a chemically induced phase transition.

Vice versa, the structure of diamond nanoclusters with unpassivated surface is exposed to surface effects that cause the graphitization process, or the transformation of the outer carbon layers to graphene.^{30,31} This effect leads to the instability of diamond films containing few atomic layers and

their transformation to multilayered graphene.^{28,32} It makes investigation of the functionalization process of diamond nanofilms especially important.

In this work, we studied in detail the formation of diamond films of nanometer thickness from single, bi-, and three-layered graphene functionalized by various adatoms and molecular groups, and estimated the external conditions for formation of different conformers. We established the connection of the surface functionalization type, structure, and surface orientation of the films. We proved that, depending on the type of adsorbed atoms and the external conditions, either chair or boat conformers can be formed from the single-layered graphene, whereas bi- and three-layered graphene can be connected to either diamond films with (110) and (111) surfaces or hexagonal diamond (lonsdaleite) films with (1010) and (2110) surfaces. These results as well as calculated potential barriers of chemisorption allow one to estimate the conditions of functionalization and stability of the diamond films with different functionalized surface. Finally, we studied the electronic properties of the films, and found a pronounced dependence of band structure and the band gap behavior on the surface functionalization and film thickness.

Received: October 15, 2014

Revised: January 9, 2015

Published: January 9, 2015

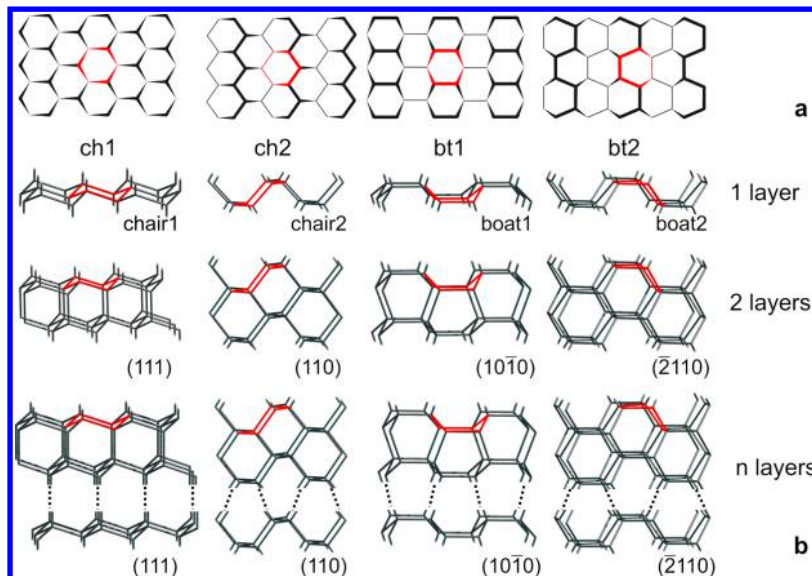


Figure 1. (a) Top perspective drawing view and (b) side view scheme and labeling of functionalized single, bi-, and n -layered diamond films. The cyclohexane-type building unit is marked by red. In common notation, single-layered functionalized graphenes are denoted by a conformer name, whereas thicker diamond films are defined by orientation of the surface.

■ COMPUTATIONAL DETAILS

All calculations of atomic and electronic structures of graphene conformers were performed using a density functional theory^{33,34} within the PBE-PAW approximation³⁵ with the periodic boundary conditions using a Vienna Ab-initio Simulation Package.^{36–38} The plane-wave energy cutoff was equal to 520 eV. To calculate the equilibrium atomic structures, the Brillouin zone was sampled according to the Monkhorst–Pack³⁹ scheme with a grid from $12 \times 12 \times 1$ to $6 \times 6 \times 1$ k -point depending on the lateral size of the unit cell of the structure. To avoid the interaction between the neighboring graphene layers, the vacuum space between them was greater than 15 Å. The structural relaxation was performed until the forces acting on each atom were less than 0.01 eV/Å.

For estimation of potential energy curves for the transition from one-, bi-, and three-layer graphene with functionalized surface to diamond films, we made step-by-step calculation of adatoms adsorption along with diamond film formation. The initial structure was n -layered graphene ($n = 1–3$) and isolated atoms/molecules distanced from its surface on 6.5 Å. The potential energy curves were calculated by gradual moving of the atoms toward the graphene surface with atomic geometry optimization of the whole structure (except fixed coordinates on c axis of adatoms and single atom on the surface) on each step until the diamond films' formation.

The C–F bond length in CF, C₂F, and C₃F films is covalent in character (1.38 Å) and agrees very well with both experimental (1.41 Å)^{10,11} and theoretical (1.37 Å)¹² values. The C–H bond length in investigation of diamond films is 1.10 Å, and is also in agreement with both experimental³ and theoretical^{3–6} values. The average computed C–C bond lengths in diamond films are a little bit longer (1.56 Å) than experimental (1.53 Å)¹⁰ and theoretical (1.55 Å)¹² values in fluorographene and diamond.

■ RESULTS AND DISCUSSION

Here, we considered different conformers of the functionalized single-, bi-, and three-layered graphene. Different conformers

represent the films with various surface orientation and atomic structure (cubic and hexagonal diamond); see Figure 1.

While benzene is the elementary unit of the graphene structure, cyclohexane can be considered as the building block of the single-layered hydrogenated graphene (graphane). The conformers of cyclohexane dictate the conformers of graphane. The low-energy “chair” conformer of cyclohexane corresponds to two graphane conformers: “chair1”⁴⁰ (usually referred to simply as “chair”) and “chair2”⁴⁰ (“washboard”,⁴¹ “stirrup”,⁴² “zigzag”⁴³), whereas the “boat” conformer corresponds to two more graphane conformers: “boat1”⁴⁰ (“bed”,⁴¹ “boat”^{42,43}) and “boat2”⁴⁰ (“armchair”⁴³). It should be noted that the terminology is applicable not only for hydrogenated graphene, but also for sp³-bounded graphene with other functionalization types (fluorographene, etc.).

All of these configurations can be considered as the first members of the diamond films families with various crystallographic orientations of the surface. The functionalized graphene of “chair1” and “chair2” conformations belongs to the group of cubic diamond films with (111) and (110) surfaces with diamond in the infinite thickness limit, whereas the “boat1” and “boat2” conformations are the first members of hexagonal diamond films with the (10̄10) and (2̄110) surface series, which are terminated by bulk lonsdaleite (Figure 1).³²

Various conformers display different energy stability, which is due to the related stability of the surfaces in the bulk state. Thus, we can talk about an important link between the structural chemistry of isomers and the chemistry of solid surfaces and nanomaterials. In this regard, the experimental control over the graphene functionalization is quite important for further technological applications.

The chemically induced phase transition opens the way to form the new structures from multilayered graphene. This effect is confirmed in a number of experimental papers in which functionalization of graphene,^{7,8,20} graphite,^{10,21} and amorphous carbon^{44,45} results in diamondization. The process of chemical diamondization can be represented as follows: chemisorption of adatom on a carbon atom changes the hybridization from sp² to sp³ and leads to an increase in the

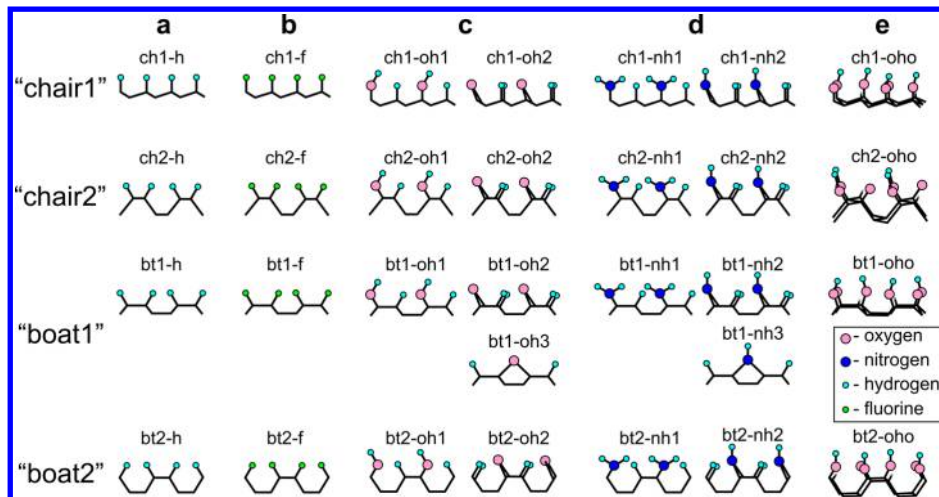


Figure 2. Scheme and labeling of the hydrogen (a), fluorine (b), water (c), ammonia (d), and combined water and oxygen (e) functionalized graphene considered in this study. Hydrogen, fluorine, oxygen, and nitrogen atoms are the circles filled by cyan, green, pink, and blue colors, while the carbon atoms are not explicitly represented.

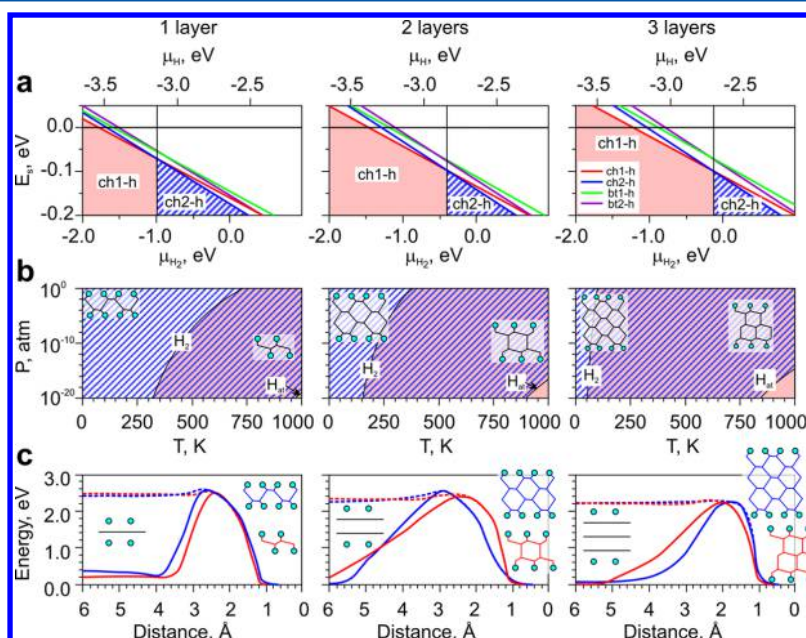


Figure 3. (a) Formation energies versus chemical potential for the different conformers of hydrogenated diamond films. The alternative bottom (top) axes show the value of chemical potential of molecular (atomic) hydrogen. (b) Phase diagrams (P, T) of stability of the hydrogenated diamond films. (c) Potential energy curves show the transition from one-, bi-, and three-layer graphene with hydrogenated surface into diamond films (chosen as zero energy level). All energies are plotted versus the average length of surface C–H bond. The schematics at the inset illustrate the initial and final structures. The potential energies for binding the molecular and atomic hydrogen are marked by solid and dashed lines, respectively.

chemical activity of the neighbored C atoms. Because of the change of hybridization, atoms go out of the plane and tend to connect with other adatoms or carbon atoms from another layer, which leads to the sp^3 -hybridized region expansion.

It should be noted that the adatoms adsorption in various arrangement leads to a formation of different conformations. In refs 41,46, the researchers obtained that the structure of the graphane/fluorographene surface can contain several phases divided by a grain boundary. Thermodynamically, different conformers display various formation energies, and, therefore, it can be supposed that the control over the adatoms organization on the graphene surface can allow one to synthesize the ultrathin diamond films with defined properties.

In this study, we considered several types of graphene functionalization most widely used in the experimental studies, such as hydrogen,^{3,7–9} fluorine,^{10,16,17} water,^{20–23} and ammonia; see Figure 2.

The formation energy of the graphene surface functionalization was estimated by the following equation:^{47,48}

$$E_s = \frac{E_{\text{tot}} - n_{\text{ad}}E_{\text{ad}} - n_{\text{C}}E_{\text{C}}}{2S} - \frac{n_{\text{ad}}}{2S}\mu_{\text{ad}}(T, p_{\text{ad}}^{\circ}) \quad (1)$$

Here, the first part of the difference is the zero-temperature surface energy (per unit area); the last part is the chemical potential of the source of adatoms (or molecular groups) depending on the temperature, T , partial pressure, p_{ad} , and implicitly on the adatoms (molecular groups) concentration.

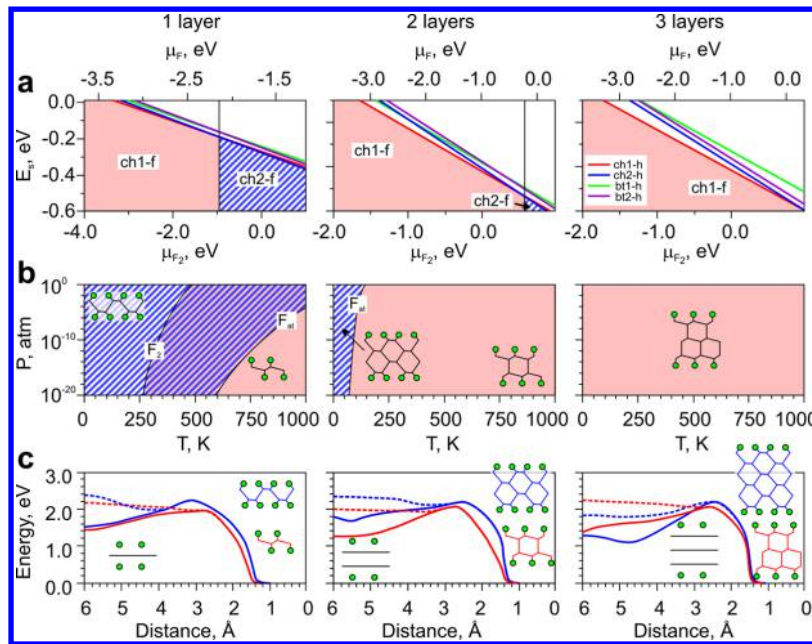


Figure 4. (a) Formation energies versus chemical potential for the different conformers of fluorinated diamond films. The alternative bottom (top) axes show the value of chemical potential of molecular (atomic) fluorine. (b) Phase diagrams (P, T) of stability of the fluorinated diamond films. (c) Potential energy curves show the transition from one-, bi-, and three-layer graphene with hydrogenated surface into diamond films (chosen as zero energy level). All energies are plotted versus the average length of surface C–F bond. The schematics at the inset illustrate the initial and final structures. The potential energies for binding the molecular and atomic fluorine are marked by solid and dashed lines, respectively.

Using this relation, it is possible to estimate the reliable conditions of functionalized surface formation.

E_{tot} is the total energy of system, E_{ad} is the energy of one adatom in case of hydrogen/fluorine or energy of adsorbed molecules in case of water/ammonia, E_C is the energy of carbon in clean graphene, S is the functionalized graphene area (this term is doubled because the graphene slab is accessed for the adsorption from both sides), n_{ad} is the number of adatoms or molecular groups, and n_C is the number of carbons in the system. $\mu_{\text{ad}}(T, p_{\text{ad}}^{\circ})$ is the chemical potential of an adatom or adsorbed molecule at given temperature and pressure, which can be calculated by the formula:

$$\mu_{\text{ad}}(T, p_{\text{ad}}^{\circ}) = \Delta H - T \Delta S + \frac{1}{2} kT \ln(x) \quad (2)$$

where ΔH and ΔS are the differences of enthalpy and entropy of the given temperature and the zero one, the values of which were obtained from the reference table,⁴⁹ x is mole fraction, amount of the given constituent divided by the total amount of all constituents in a mixture or, in the case of gas, a ratio of constituent partial pressure p_{ad}° to the total pressure of system P , $x = p_{\text{ad}}^{\circ}/P$. Decrease of the chemical potential in the absolute magnitude (which is equal to a constituent concentration increase) leads to a decline of E_s ; that is, the formation of the system became more preferable. Thus, it is possible to find the energy-favorable structure for the chosen value of the chemical potential, based on a comparison of the energies of formation of various functionalized diamond films with different structures and surfaces.

Because the value of the chemical potential depends on the temperature and pressure, it is also possible to obtain a phase diagram (P, T), which will establish the area of stability of specific diamond film. In the presented phase diagrams, the results for the limiting case of pure gas functionalization $x = 1$ (the system has no external substances, $P = p_{\text{ad}}^{\circ}$), but these data

can be easily extended to the $x < 1$ case. Note that at absolute zero temperature, $\mu_{\text{ad}} = 0$ and E_s equals pure formation energy per area unit in the DFT gauge.

HYDROGEN AND FLUORINE

At first, we consider the hydrogenated diamond films' formation; see Figure 3. Surface formation energy for all of the considered conformers is negative for this case (Figure 3a), which means that graphene functionalized by hydrogen in all conformers should form spontaneously, but conformers ch1 and ch2 are energy favorable at different environmental conditions.

It should be noted that in our analysis at $\mu_{\text{ad}} = 0$, E_s equals pure formation energy per area unit from DFT calculation. Therefore, we do not consider the region at $\mu_{\text{ad}} > 0$ on the formation energies versus chemical potential graphs. Yet the upper axes are not starting from zero because the behavior of the structure does not change within increasing chemical potential; for example, for Figure 3a in the case of three-layered structure for chemical potential of atomic hydrogen above -2.5 eV, structure ch2-h will be more stable than others up to $\mu_H = 0$.

The increasing number of graphene layers leads to a shift of crossing point between ch1 and ch2 conformers inside the ch2 formation region, which is represented by decreasing ch2 energy-favorable area in the (P, T) diagram (Figure 3b). From these data, it can be concluded that the molecular hydrogen adsorption to multilayered graphene at a broad range of temperatures and pressures will lead to the formation of films with (111) surface. However, the high barrier of chemisorption by H_2 (>2 eV) makes the process of hydrogenation difficult (Figure 3c).

The experimental synthesis of hydrogenated graphene is realized by cold hydrogen plasma exposure.^{3,50} We simulated this process by using atomic hydrogen as a source for the

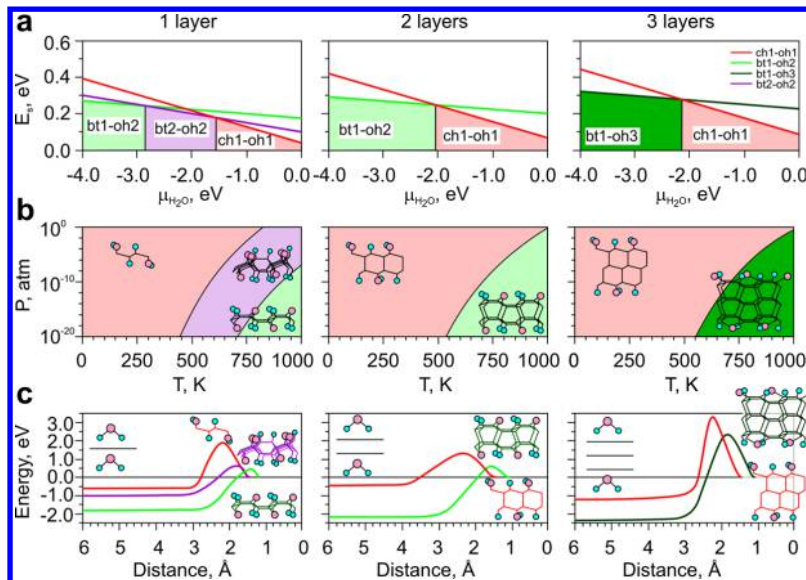


Figure 5. (a) Formation energies versus chemical potential of H_2O for the different conformers of water-functionalized diamond films. (b) Phase diagrams (P,T) of stability of the water-functionalized diamond films. (c) Potential energy curves show the transition from one-, bi-, and three-layer graphene with water-functionalized surface into diamond films (chosen as zero energy level). All energies are plotted versus the average length of surface C–O bond. The schematics at the inset illustrate the initial and final structures.

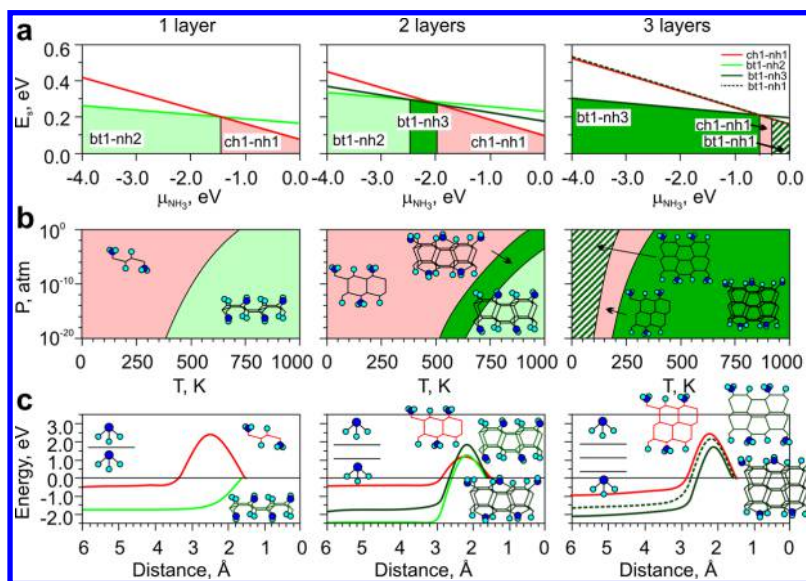


Figure 6. (a) Formation energies versus chemical potential of NH_3 for the different conformers of ammonia-functionalized diamond films. (b) Phase diagrams (P,T) of stability of the ammonia-functionalized diamond films. (c) Potential energy curves show the transition from one-, bi-, and three-layer graphene with ammonia-functionalized surface into diamond films (chosen as zero energy level). All energies are plotted versus the average length of surface C–N bond. The schematics at the inset illustrate the initial and final structures.

hydrogenation of graphene surface. The high activity of hydrogen atoms vanishes the potential barrier of hydrogenation, which facilitates formation of C–H bonds (Figure 3c). Thermodynamic parameters of such process can be estimated from eq 1 by using the chemical potential of atomic hydrogen, $\mu_H(T,P)$. In this case, the ch1/ch2 crossing point, Figure 3a (equilibrium (P,T) line, Figure 3b), is located in a lower chemical potential value (higher temperature range). Therefore, for at least up to three-layered diamond films, both ch1 and ch2 conformers can be realized depending on the environmental conditions.

In case of fluorinated diamond films, the situation is qualitatively the same (Figure 4), but the region of ch2 stability

decreases with a rise in the number of layers much faster than in the previous case. Whereas in the case of single-layered film the ch1/ch2 crossing point (Figure 4a) is located at $\mu_{F_2}(T,P) = -0.95$ eV ($\mu_F(T,P) = -2.14$ eV), for the two-layer films this point is located in the positive chemical potential range for molecular fluorine ($\mu_{F_2}(T,P) = 2.93$ eV), which means that chemisorption of molecular fluorine can form only the “chair” (ch1) conformer. Moreover, in the case of thicker films, both F and F_2 chemisorption lead to formation of ch1 conformer only (therefore, in Figure 4b only the ch1 region is shown for three-layered structure, and just one equilibrium (P,T) line (for atomic fluorine) is present for two-layered structure).

This result is supported by experiment, as in refs 10,21, graphite fluoride was investigated, and it was shown that this material has a hexagonal symmetry along the *c* axis. As was shown in ref 16 (and in the later study¹⁷), the fluorination at high temperature (between 600 and 900 K) generates two types of covalent fluorinated graphite with $(C_2F)_n$ and $(CF)_n$ structural types, with a hexagonal symmetry as well. In refs 51 and 52, the hexagonal graphite fluorite with a composition of CF_x ($0.5 < x < 1$) was prepared at a pressure of fluorine F_2 of $P = 0.1\text{--}1$ atm ($x = 1$) and temperature $T = 650\text{--}875$ K. These experimental results also are in accord with our theoretical estimations.

The main difference between hydrogen and fluorine functionalization is a larger chemical activity of the fluorine molecule, which much more easily dissociates to the atoms than hydrogen molecule. Therefore, the fluorination is a lower-cost energy process than hydrogenation (Figure 4c). Even molecular fluorine can be decomposed and bind to graphene with an energy barrier of less than 1 eV. The fact of an easier synthesis of fluorographene than graphane is supported by previous theoretical⁵³ and experimental data.^{54–56}

■ WATER AND AMMONIA

Besides hydrogen and fluorine, we considered diamond film conformers functionalized by water and ammonia. This part was initiated by recent experimental results²⁰ where the multilayered graphene diamondization by binding to the surface carbon atoms with hydroxyl groups was reported.

To limit our study, we considered only the structures in which the ratio of oxygen(nitrogen) atoms to hydrogen atoms corresponds to the ratio in water(ammonia) molecules; that is, the content of oxygen and hydrogen was always O:H = 1:2 in the case of graphene functionalized by water, and N:H = 1:3 in the case of graphene functionalized by ammonia. In the considered cases, the surface formation energies of single-, bi-, and three-layer functionalized graphene in water and ammonia atmospheres are always positive (Figures 5 and 6), which means that graphene would not spontaneously form a diamond film in this atmosphere. This result corresponds to the data from ref 20, where the multilayered graphene diamondization occurred under the influence of pressure-dependent charge injection experiment with binding of the oxygen functional groups to the surface.

At normal conditions ($P = 1$ atm, $T = 298$ K), ch1 (ch1-oh1) is the most stable configuration for single-, bi-, and three-layered films. Yet in contrast with previous considered cases for the high values of chemical potential films, the bt1 conformer (with hexagonal diamond structure) becomes energy favorable. For the case of a single-layered water-functionalized graphene, the phase diagram (P, T) consists of three parts (Figure 5b): in addition to ch1 conformer (ch1-oh1), bt1 (bt1-oh2) and bt2 (bt2-oh2) configurations are presented (Figure 2c). The bt1-oh2 is the most stable configuration at a high temperature for single- and bilayered films, but displays low barrier (<0.6 eV) for detachment of O- and H-groups from the surface, which manifests the low stability of such hexagonal diamond films.

For a three-layered graphene, bt1-oh3 became favorable in this phase diagram region. Instead of as in previous cases, high potential barrier prevents breaking of C–H and C–O bonds and therefore hinders the process graphitization of the films.

The (P, T) diagram of a single-layered water-functionalized graphene also contains a region of bt2-oh2 formation. This structure is stable only in the flexible single-layer configuration,

because the bounded oxygen bridge pulls together the neighboring carbon atoms. The relaxed geometry of the bt2-oh2 structure is not pure “boat” conformation, but contains a “half-chair” conformation as well (a transitional form between the “chair” and the “boat”) generated by the deformed six-member rings. In the cases of bi- and three-layered graphene, this conformer displays a higher energy and is not present in the corresponding phase diagrams.

Graphene in ammonia atmosphere can also form the “chair” and the “boat” conformations (Figure 6). The phase diagram of the functionalized single and bilayered graphene along with ch1 (ch1-nh1) conformer contains also a bt1 (bt1-nh2) configuration. Yet the last configuration has no potential barrier for desorption of ammonia for the single-layered functionalized graphene, whereas ch1-nh1 has a barrier >1 eV for chemisorption reaction for single-, bi-, and three-layered films (Figure 6c).

Beginning from the bilayered sp^3 -hybridized films, the phase diagram displays the third formation region of bt1 (bt1-nh3), which differs from bt1-nh2 by the –NH group position (Figure 2d). In the case of three-layered film, the bt1-nh3 fills a large part of the diagram with acquisition of a new part of bt1-nh1 along with decreasing the ch1 conformer contribution. Therefore, we can expect the formation of almost only hexagonal diamond films from the adsorption of ammonia groups to the three-layered structures; bilayered diamond film can contain both ch1 and bt1 conformers, and single-layered ammonia-functionalized graphene should display only one ch1-nh1 configuration.

For our final consideration of the functionalized multilayered graphene formation, we analyze the mixed H_2O and O_2 type of graphene surface functionalization. According to the early paper²¹ where the structure of graphite oxide layer was proposed as a diamond film with the surface functionalized by –OH and –O-groups in composition $C_8O_3H_2$ (the intermediate form between $C_8(OH)_4$ and C_8O_2), we consider this system as $C_8O_2(H_2O)$. In correspondence with this, in the thermodynamic analysis, we use two chemical potentials μ_{O_2} and μ_{H_2O} , which determine the formation energy of the functionalized graphene surface in the following way:

$$E_s = \frac{1}{2S}(E_{tot} - n_{O_2}E_{O_2} - n_{H_2O}E_{H_2O} - n_C E_C) \\ - \frac{n_{O_2}}{2S}\mu_{O_2}(T, P) - \frac{n_{H_2O}}{2S}\mu_{H_2O}(T, P) \quad (3)$$

Here, E_{O_2} and E_{H_2O} are energies of oxygen and water molecules, respectively, whereas n_{O_2} and n_{H_2O} are their quantities in a unit cell. $\mu_{O_2}(T, P)$ and $\mu_{H_2O}(T, P)$ are the chemical potentials of oxygen and vapor of water, respectively. This chemical potential can be calculated using the formula 2 by substituting the appropriate values by $\Delta H(H_2O)$, $\Delta S(H_2O)$, $\Delta H(O_2)$, and $\Delta S(O_2)$, the values of which were obtained from the reference table.⁴⁹

Like in the previous cases, we considered single- ($C_4O_2(H_2O)$), bi- ($C_8O_2(H_2O)$), and three-layered ($C_{12}O_2(H_2O)$) diamond films (among which a bilayered diamond film corresponds to the model proposed in ref 21). In the case of a single-layered functionalized graphene, no conformers survived after the relaxation. The thicker films display several stable conformers, the surface formation energies of which we compared in Figure 7. The formation

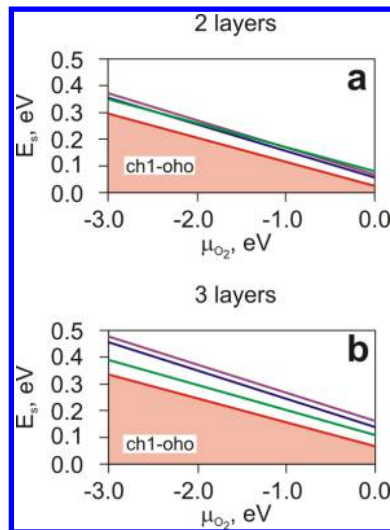


Figure 7. Surface formation energies versus chemical potential of various conformers of water- and oxygen-functionalized (a) bi- and (b) three-layered diamond films.

energies of those structures are positive, which indicates that the structures cannot be formed spontaneously. The most stable conformer in both bi- and three-layered sp^3 -hybridized films is the ch1 (ch1-oho) one in the whole range of temperatures and pressures in contrast with pure H_2O surface functionalization. For the case of bilayered diamond films, our result confirms the prediction of ref 21.

ELECTRONIC STRUCTURE

In addition to the thermodynamic description of films formation, we analyzed the electronic structure of the films considered in this study. It was found that the location of the valence band top and the conduction band bottom depends both on the film thickness and on the functionalization type (Table 1, Supporting Information Table 1S). Films with the surface functionalized by H, ammonia (except the case of bt1-nh1), and water (only in the case of ch1-oh1) display a direct band gap, E_{gap} , and its value decreases with a film thickness

increase. In the case of the hydrogenated films, this result is consistent with the available reference data for the ch1 configuration.^{24,27,57}

In the case of fluorinated films, the transition from direct to indirect E_{gap} at the three-layered ch2-f was observed. This result corresponds with ref 58, where the same transition was found for the four-layered ch1-f. In opposition to the previous cases, the fluorinated ch1 and ch2 films exhibit a growing behavior of the band gap, in accordance with ref 58.

Water-functionalized films in bt1 and bt2 configurations are indirect semiconductors with a valence band top location at the Γ point, and the conduction band bottom between Γ and X for the single-layered bt1-oh2, bt2-oh2, and at X point for bi- and three-layered films of bt1-oh2 and bt1-oh3 configurations.

The combined water- and oxygen-functionalized bi- and three-layered diamond films ch1-oho display a metallic state due to the unsaturated surface carbon atoms (see Figure 2e). This fact raises doubts in the model proposed in ref 21, because the semiconducting behavior of graphite oxide was normally observed in the experiments.⁵⁹

The atomic and electronic structures for all of the energy-favorable films can be found in the Supporting Information. We can conclude that the features of the electronic properties of the films can be modified to a considerable degree by the graphene functionalization type that can allow one to obtain two-dimensional materials with tunable electronic properties in a chemical way.

CONCLUSIONS

In this Article, we focused on the properties of single-, bi-, and three-layered diamond films of nanometer thickness with surface functionalized by different groups. We found that depending on the external conditions (temperature, T , pressure, P , and concentration of gas used for the functionalization, x), it is possible to obtain a number of conformers with different properties. Calculations of phase diagram (P,T) for $x = 1$ at different external pressures allow one to directly visualize the regions of the most stable conformers. Functionalization by hydrogen and fluorine allows one to obtain films of ch1 and ch2 conformers, whereas water and ammonia adsorption leads to a more complex situation. In the case of water vapor functionalization, it was found that besides ch1, the bt1 conformers can be fabricated. Adsorption of ammonia also allows one to obtain both ch1 and bt1 configurations. In addition, we considered the films with the surface functionalized by $-OH$ and $-O-$ groups, and found that ch1 is stable in the whole range of temperatures and pressures. Finally, various behavior of the electronic structure of the energy-favorable films depending on the film thickness was analyzed. Our results are supported by the existing theoretical and experimental data and allow one to open the way to synthesized graphene-based nanostructures with tunable electronic properties.

ASSOCIATED CONTENT

Supporting Information

Description of eqs 2 and 3, and the band structure and geometry for most stable conformers. This material is available free of charge via the Internet at <http://pubs.acs.org>.

AUTHOR INFORMATION

Corresponding Author

*E-mail: pbsorokin@tisnum.ru.

^aIndirect band gap.

Notes

The authors declare no competing financial interest.

ACKNOWLEDGMENTS

We acknowledge Prof. David Tománek for hospitality and fruitful discussions. We are grateful to the “Chebyshev” and “Lomonosov” supercomputers of the Moscow State University for the possibility of using a cluster computer for our quantum-chemical calculations. Part of the calculations was made on the Joint Supercomputer Center of the Russian Academy of Sciences. This work was supported by the Ministry of Education and Science of the Russian Federation (contract no. 14.B37.21.1645) and Russian Foundation for Basic Research (contract no. 12-02-31261/13).

REFERENCES

- (1) Novoselov, K. S.; Jiang, D.; Schedin, F.; Booth, T. J.; Khotkevich, V. V.; Morozov, S. V.; Geim, A. K. Two-dimensional Atomic Crystals. *Proc. Natl. Acad. Sci. U.S.A.* **2005**, *102*, 10451–10453.
- (2) Castro Neto, A. H.; Guinea, F.; Peres, N. M. R.; Novoselov, K. S.; Geim, A. K. The Electronic Properties of Graphene. *Rev. Mod. Phys.* **2009**, *81*, 109–162.
- (3) Elias, D. C.; Nair, R. R.; Mohiuddin, T. M. G.; Morozov, S. V.; Blake, P.; Halsall, M. P.; Ferrari, A. C.; Boukhvalov, D. W.; Katsnelson, M. I.; Geim, A. K.; et al. Control of Graphene’s Properties by Reversible Hydrogenation: Evidence for Graphane. *Science* **2009**, *323*, 610–613.
- (4) Boukhvalov, D. W.; Katsnelson, M. I. Chemical Functionalization of Graphene. *J. Phys.: Condens. Matter* **2009**, *21*, 344205.
- (5) Sofo, J. O.; Chaudhari, A. S.; Barber, G. D. Graphane: a Two-dimensional Hydrocarbon. *Phys. Rev. B* **2007**, *75*, 153401(4).
- (6) Boukhvalov, D.; Katsnelson, M.; Lichtenstein, A. Hydrogen on Graphene: Electronic Structure, Total Energy, Structural Distortions and Magnetism from First-principles Calculations. *Phys. Rev. B* **2008**, *77*, 035427.
- (7) Odkhuu, D.; Shin, D.; Ruoff, R. S.; Park, N. Conversion of Multilayer Graphene into Continuous Ultrathin sp^3 -bonded Carbon Films on Metal Surfaces. *Sci. Rep.* **2013**, *3*, 3276.
- (8) Rajasekaran, S.; Abild-Pedersen, F.; Ogasawara, H.; Nilsson, A.; Kaya, S. Interlayer Carbon Bond Formation Induced by Hydrogen Adsorption in Few-layer Supported Graphene. *Phys. Rev. Lett.* **2013**, *111*, 085503.
- (9) Arnault, J. C.; Petit, T.; Girard, H.; Chavanne, A.; Gesset, C.; Sennour, M.; Chaigneau, M. Surface Chemical Modifications and Surface Reactivity of Nanodiamonds Hydrogenated by CVD Plasma. *Phys. Chem. Chem. Phys.* **2011**, *13*, 11481–11487.
- (10) Touhara, H.; Kadono, K.; Fujii, Y.; Watanabe, N. On the Structure of Graphite Fluoride. *Z. Anorg. Allg. Chem.* **1987**, *544*, 7–20.
- (11) Mahajan, V. K.; Badachhape, R. B.; Margrave, J. L. X-ray Powder Diffraction Study of poly(carbon monofluoride), $CF_{1.12}$. *Inorg. Nucl. Chem. Lett.* **1974**, *10*, 1103–1109.
- (12) Charlier, J. C.; Gonze, X.; Michenaud, J. P. First-principles Study of Graphite Monofluoride (CF_n). *Phys. Rev. B* **1993**, *47*, 16162–16168.
- (13) Santos, H.; Henrard, L. Fluorine Adsorption on Single and Bilayer Graphene: Role of Sublattice and Layer Decoupling. *J. Phys. Chem. C* **2014**, *118*, 27074–27080.
- (14) Robinson, J. T.; Burgess, J. S.; Junkermeier, C. E.; Badescu, S. C.; Reinecke, T. L.; Perkins, F. K.; Zalalutdinov, M. K.; Baldwin, J. W.; Culbertson, J. C.; Sheehan, P. E.; et al. Properties of Fluorinated Graphene Films. *Nano Lett.* **2010**, *10*, 3001–3005.
- (15) Liu, H. Y.; Hou, Z. F.; Hu, C. H.; Yang, Y.; Zhu, Z. Z. Electronic and Magnetic Properties of Fluorinated Graphene with Different Coverage of Fluorine. *J. Phys. Chem. C* **2012**, *116*, 18193–18201.
- (16) Touhara, H.; Okino, F. Property Control of Carbon Materials by Fluorination. *Carbon* **2000**, *38*, 241–267.
- (17) Ahmad, Y.; Dubois, M.; Gurin, K.; Hamwi, A.; Fawal, Z.; Kharitonov, A. P.; Generalov, A. V.; Klyushin, A. Y.; Simonov, K. A.; Vinogradov, N. A.; et al. NMR and NEXAFS Study of Various Graphite Fluorides. *J. Phys. Chem. C* **2013**, *117*, 13564–13572.
- (18) Peng, Y.; Li, J. Ammonia Adsorption on Graphene and Graphene Oxide: a First-principles Study. *Front. Environ. Sci. Eng.* **2013**, *7*, 403–411.
- (19) Seyed-Talebi, S. M.; Beheshtian, J. Computational Study of Ammonia Adsorption on the Perfect and Rippled Graphene Sheet. *Phys. B (Amsterdam, Neth.)* **2013**, *429*, 52–56.
- (20) Barboza, A. P. M.; Guimaraes, M. H. D.; Massote, D. V. P.; Campos, L. C.; Neto, N. M. B.; Cancado, L. G.; Lacerda, R. G.; Chacham, H.; Mazzoni, M. S. C.; Neves, B. R. A. Room-temperature Compression-induced Diamondization of Few-layer Graphene. *Adv. Mater.* **2011**, *23*, 3014–3017.
- (21) Nakajima, T.; Mabuchi, A.; Hagiwara, R. A New Structure Model of Graphite Oxide. *Carbon* **1988**, *26*, 357–361.
- (22) He, H.; Klinowski, J.; Forster, M.; Lerf, A. A New Structural Model for Graphite Oxide. *Chem. Phys. Lett.* **1998**, *287*, 53–56.
- (23) Böttcher, S.; Weser, M.; Dedkov, Y. S.; Horn, K.; Voloshina, E. N.; Paulus, B. Graphene on Ferromagnetic Surfaces and Its Functionalization with Water and Ammonia. *Nanoscale Res. Lett.* **2011**, *6*, 214.
- (24) Chernozatonskii, L. A.; Sorokin, P. B.; Kuzubov, A. A.; Sorokin, B. P.; Kvashnin, A. G.; Kvashnin, D. G.; Avramov, P. V.; Yakobson, B. I. Influence of Size Effect on the Electronic and Elastic Properties of Diamond Films with Nanometer Thickness. *J. Phys. Chem. C* **2011**, *115*, 132–136.
- (25) Chernozatonskii, L. A.; Sorokin, P. B.; Kvashnin, A. G.; Kvashnin, D. G. Diamond-like C_2H Nanolayer, Diamane: Simulation of the Structure and Properties. *JETP Lett.* **2009**, *90*, 134–138.
- (26) Leenaerts, O.; Partoens, B.; Peeters, F. M. Hydrogenation of Bilayer Graphene and the Formation of Bilayer Graphane from First Principles. *Phys. Rev. B* **2009**, *80*, 245422.
- (27) Zhu, L.; Hu, H.; Chen, Q.; Wang, S.; Wang, J.; Ding, F. Formation and Electronic Properties of Hydrogenated Few Layer Graphene. *Nanotechnology* **2011**, *22*, 185202.
- (28) Kvashnin, A. G.; Chernozatonskii, L. A.; Yakobson, B. I.; Sorokin, P. B. Phase Diagram of Quasi-two-dimensional Carbon, from Graphene to Diamond. *Nano Lett.* **2014**, *14*, 676–681.
- (29) Bonis, A. D.; Curcio, M.; Santagata, A.; Rau, J.; Galasso, A.; Teghil, R. Fullerene-reduced Graphene Oxide Composites Obtained by Ultrashort Laser Ablation of Fullerite in Water. *Appl. Surf. Sci.*, in press.
- (30) Kuznetsov, V. L.; Butenko, Y. V. Nanodiamond Graphitization and Properties of Onion-like Carbon. *Ultrananocryst. Diamond* **2005**, 199–216.
- (31) Shang, N.; Papakonstantinou, P.; Wang, P.; Zakharov, A.; Palnitkar, U.; Lin, I. N.; Chu, M.; Stamboulis, A. Self-assembled Growth, Microstructure, and Field-emission High-performance of Ultrathin Diamond Nanorods. *ACS Nano* **2009**, *3*, 1032–1038.
- (32) Kvashnin, A. G.; Sorokin, P. B. Lonsdaleite Films with Nanometer Thickness. *J. Phys. Chem. Lett.* **2014**, *5*, 541–548.
- (33) Hohenberg, P.; Kohn, W. Inhomogeneous Electron Gas. *Phys. Rev.* **1964**, *136*, 864–871.
- (34) Kohn, W.; Sham, L. J. Self-consistent Equations Including Exchange and Correlation Effects. *Phys. Rev.* **1965**, *140*, 1133–1138.
- (35) Perdew, J. P.; Burke, K.; Ernzerhof, M. Generalized Gradient Approximation Made Simple. *Phys. Rev. Lett.* **1996**, *77*, 3865–3868.
- (36) Kresse, G.; Hafner, J. Ab Initio Molecular Dynamics for Liquid Metals. *Phys. Rev. B* **1993**, *47*, 558–561.
- (37) Kresse, G.; Hafner, J. Ab Initio Molecular-dynamics Simulation of the Liquid-metal–amorphous-semiconductor Transition in Germanium. *Phys. Rev. B* **1994**, *49*, 14251–14269.
- (38) Kresse, G.; Furthmüller, J. Efficient Iterative Schemes for Ab Initio Total-energy Calculations Using a Plane-wave Basis Set. *Phys. Rev. B* **1996**, *54*, 11169–11186.
- (39) Monkhorst, H. J.; Pack, J. D. Special Points for Brillouin-zone Integrations. *Phys. Rev. B* **1976**, *13*, 5188–5192.

- (40) Wen, X. D.; Hand, L.; Labet, V.; Yang, T.; Hoffmann, R.; Ashcroft, N. W.; Oganov, A. R.; Lyakhov, A. O. Graphane Sheets and Crystals Under Pressure. *Proc. Natl. Acad. Sci. U.S.A.* **2011**, *108*, 6833–6837.
- (41) Artyukhov, V. I.; Chernozatonskii, L. A. Structure and Layer Interaction in Carbon Monofluoride and Graphane: a Comparative Computational Study. *J. Phys. Chem. A* **2010**, *114*, 5389–5396.
- (42) Bhattacharya, A.; Bhattacharya, S.; Majumder, C.; Das, G. Third Conformer of Graphane: a First-principles Density Functional Theory Study. *Phys. Rev. B* **2011**, *83*, 033404.
- (43) Leenaerts, O.; Peelaers, H.; Hernández-Nieves, A. D.; Partoens, B.; Peeters, F. M. First-principles Investigation of Graphene Fluoride and Graphane. *Phys. Rev. B* **2010**, *82*, 195436.
- (44) Lifshitz, Y.; Köhler, T.; Frauenheim, T.; Guzmann, I.; Hoffman, A.; Zhang, R. Q.; Zhou, X. T.; Lee, S. T. The Mechanism of Diamond Nucleation from Energetic Species. *Science* **2002**, *297*, 1531–1533.
- (45) Sun, Y.; Kvashnin, A. G.; Sorokin, P. B.; Yakobson, B. I.; Billups, W. E. Radiation-induced Nucleation of Diamond from Amorphous Carbon: Effect of Hydrogen. *J. Phys. Chem. Lett.* **2014**, *5*, 1924–1928.
- (46) Flores, M. Z. S.; Autreto, P. A. S.; Legoa, S. B.; Galvao, D. S. Graphene to Graphane: a Theoretical Study. *Nanotechnology* **2009**, *20*, 465704.
- (47) Wassmann, T.; Seitsonen, A. P.; Saitta, A. M.; Lazzeri, M.; Mauri, F. Structure, Stability, Edge States, and Aromaticity of Graphene Ribbons. *Phys. Rev. Lett.* **2008**, *101*, 096402(4).
- (48) Mukhopadhyay, S.; Bailey, C. L.; Wander, A.; Searle, B. G.; Muryn, C. A.; Schroeder, S. L. M.; Lindsay, R.; Weiher, N.; Harrison, N. M. Stability of the AlF₃ Surface in H₂O and HF Environments: an Investigation Using Hybrid Density Functional Theory and Atomistic Thermodynamics. *Surf. Sci.* **2007**, *601*, 4433–4437.
- (49) Chase, M. W.; Davies, C. A.; Downey, J. R.; Frurip, D. J.; McDonald, R. A.; Syverud, A. N. Janaf Thermochemical Tables Third Edition. *J. Phys. Chem. Ref. Data* **1985**, *14*, 1856.
- (50) Luo, Z.; Yu, T.; Kim, K. J.; Ni, Z.; You, Y.; Lim, S.; Shen, Z.; Wang, S.; Lin, J. Thickness-dependent Reversible Hydrogenation of Graphene Layers. *ACS Nano* **2009**, *3*, 1781–1788.
- (51) Kita, Y.; Nobutsu, W.; Yukio, F. Chemical Composition and Crystal Structure of Graphite Fluoride. *J. Am. Chem. Soc.* **1979**, *101*, 3832–3841.
- (52) Watanabe, N. Two Types of Graphite Fluorides, (CF)_n and (C₂F)_n, and Discharge Characteristics and Mechanisms of Electrodes of (CF)_n and (C₂F)_n in Lithium Batteries. *Solid State Ionics* **1980**, *1*, 87–110.
- (53) Ribas, M. A.; Singh, A. K.; Sorokin, P. B.; Yakobson, B. I. Patterning Nanoroads and Quantum Dots on Fluorinated Graphene. *Nano Res.* **2011**, *4*, 143–152.
- (54) Nair, R. R.; Ren, W.; Jalil, R.; Riaz, I.; Kravets, V. G.; Britnell, L.; Blake, P.; Schedin, F.; Mayorov, A. S.; Yuan, S.; et al. Fluorographene: a Two-dimensional Counterpart of Teflon. *Small* **2010**, *6*, 2877–2884.
- (55) Jeon, K. J.; Lee, Z.; Pollak, E.; Moreschini, L.; Bostwick, A.; Park, C. M.; Mendelsberg, R.; Radmilovic, V.; Kostecki, R.; Richardson, T. J.; et al. Fluorographene: a Wide Bandgap Semiconductor with Ultraviolet Luminescence. *ACS Nano* **2011**, *5*, 1042–1046.
- (56) Cheng, S. H.; Zou, K.; Okino, F.; Gutierrez, H. R.; Gupta, A.; Shen, N.; Eklund, P. C.; Sofo, J. O.; Zhu, J. Reversible Fluorination of Graphene: Evidence of a Two-dimensional Wide Bandgap Semiconductor. *Phys. Rev. B* **2010**, *81*, 205435.
- (57) Lee, J. K.; Lee, S.; Kim, Y. I.; Kim, J. G.; Lee, K. I.; Ahn, J. P.; Min, B. K.; Yu, C. J.; Chae, K. H.; John, P. Structure of Multi-wall Carbon Nanotubes: AA' Stacked Graphene Helices. *Appl. Phys. Lett.* **2013**, *102*, 161911.
- (58) Takagi, Y.; Kusakabe, K. Transition from Direct Band Gap to Indirect Band Gap in Fluorinated Carbon. *Phys. Rev. B* **2002**, *65*, 4.
- (59) Dreyer, D. R.; Park, S.; Bielawski, C. W.; Ruoff, R. S. The Chemistry of Graphene Oxide. *Chem. Soc. Rev.* **2010**, *39*, 228–240.